Reaction Processes of O(^{1}D) with Fluoroethane Compounds

Mitsuhiko Kono† and Yutaka Matsumi*

Solar-Terrestrial Environment Laboratory, Nagoya University, Honohara 3-13, Toyokawa 442-8507, Japan

Received: May 12, 2000; In Final Form: September 26, 2000

Product branching ratios and rate constants for the O(^{3}P) atom and OH radical formation processes in the reaction of electronically excited oxygen O(^{1}D) atoms with fluoroethanes were measured at room temperature. The reactions of CHF_2-CF_3 (HFC-125), CH_2F-CF_3 (HFC-134a), CHF_2-CHF_2 (HFC-134), CH_3-CF_3 (HFC-143a), CH_2F-CHF_2 (HFC-143), and CH_3-CHF_2 (HFC-152a) were studied. Laser-induced fluorescence techniques using vacuum and near-ultraviolet lasers are applied to the detection of O(^{1}D, $^3P_2$) atoms and OH radicals, respectively. The results are compared with previous investigations, and reaction mechanisms are discussed on the basis of the present results. The rate constants for the OH radical production were proportional to the total number of H atoms included in the fluoroethane reactants, and those for the reaction processes are interpreted with the molecular structures of fluoroethane reactants.

1. Introduction

Hydrofluorocarbon (HFC) compounds are used as substitutes for the ozone-destroying chlorofluorocarbon (CFC) compounds.[1−7] However, they still have the potential to be greenhouse gases, because their radiative forcing, i.e., absorption of the infrared radiation from the earth, is significant.[7,8] Therefore, the reaction rate coefficient of HFC with O(^{1}D) atoms k_r, as well as that with OH radicals, plays the important role of controlling the atmospheric lifetime of the HFCs.[9,10] The interaction between O(^{1}D) and HFC is considered to lead to

$$\mathrm{HFC} + \mathrm{O}(^1\mathrm{D}) \rightarrow \mathrm{HFC} + \mathrm{O}(^3\mathrm{P}), \quad k_q \tag{1}$$

$$\mathrm{HFC} + \mathrm{O}(^1D) \rightarrow \mathrm{OH} + \text{products}, \quad k_{OH} \tag{2}$$

$$\mathrm{HFC} + \mathrm{O}(^1D) \rightarrow \text{Other products}, \quad k_{other} \tag{3}$$

where k_q, k_{OH}, and k_{other} are the rate constants for the physical quenching of O(^{1}D) to O(^{3}P), the chemical reactions producing OH($X\,^2\prod$), and the chemical reaction pathway(s) other than the quenching and OH formation, respectively. The total decomposition rate of an HFC is $k_r = k_{OH} + k_{other} = k_{total} - k_q$.

The total k_{total} and quenching k_q rate constants of the reaction between O(^{1}D) and the fluoromethane compounds (CHF_3, CH_2F_2, and CH_3F) were measured in our previous study.[11] The values of $k_{total} - k_q$ which we determined in the reaction with CHF_3, CH_2F_2, and CH_3F were 0.026 ± 0.013, 0.15 ± 0.08, and 1.2 ± 0.1 in units of 10^{-10} cm^3 molecule^{-1} s^{-1}, respectively. This indicates that the reaction rate constants are unambiguously related to the probability of the attack of O(^{1}D) atom on the C−H bonds. However, the reaction system between O(^{1}D) and larger HFC molecules is more complicated, i.e., (i) there are many feasible reaction pathways and (ii) the reactivity of fluoroethane probably depends on its molecular structure.

In the present study, we report the k_q, k_{OH}, and k_{other} values in the reaction of O(^{1}D) with the fluoroethane compounds by measuring the total rate coefficients for the removal of O(^{1}D), $k_{total} = k_q + k_{OH} + k_{other}$, and the quantum yields for the production of O(^{3}P), ϕ_q, and OH(X), ϕ_{OH}. These values are defined as

$$k_q = \phi_q k_{total} \tag{4}$$

$$k_{OH} = \phi_{OH} k_{total} \tag{5}$$

$$k_{other} = (1 - \phi_q - \phi_{OH}) k_{total}. \tag{6}$$

In the present experiment, the decay of O(^{1}D) and rise of O(^{3}P) were monitored to determine the k_{total} values. To measure the concentration of O(^{1}D) and O(^{3}P) produced by the physical quenching process (reaction 1), we applied the technique of time-resolved laser-induced fluorescence (LIF) detection using a vacuum UV (vuv) laser. The vuv laser wavelengths was tuned at the atomic resonance lines of the 3s ^{1}D° ← 2p ^{1}D and 3s ^{3}S° ← 2p $^3P_2$ transitions which were located at 115.22 and 130.22 nm, respectively. The OH(X) products are also detected by LIF using the OH($A^2\Sigma^+ - X\,^2\prod$; 1−0) transition around 282 nm.

2. Experimental Section

The HFC compounds studied were CHF_2-CF_3 (HFC-125), CH_2F-CF_3 (HFC-134a), CHF_2-CHF_2 (HFC-134), CH_3-CF_3 (HFC-143a), CH_2F-CHF_2 (HFC-143), and CH_3-CHF_2 (HFC-152a). The photolysis of N_2O by an ArF excimer laser (Lambda Physik, Compex) generating 193 nm radiation was used to produce O(^{1}D),[12,13]

$$N_2O + h\nu(193\ \mathrm{nm}) \rightarrow N_2 + \mathrm{O}(^1\mathrm{D}) \tag{7}$$

For each HFC reactant, the quenching quantum yield ϕ_q was obtained by measuring the relative intensity of the asymptotic

* To whom correspondence should be addressed. E-mail: matsumi@stelab.nagoya-u.ac.jp. Fax: +81-533-89-5593.

† Research School of Physical Sciences and Engineering, Australian National University, Canberra, ACT 0200, Australia.

10.1021/jp001786q CCC: $20.00
Published on Web 12/13/2000

$O(^3P)$ signal to that produced in the interaction between $O(^1D)$ and N_2,

$$N_2 + O(^1D) \rightarrow N_2 + O(^3P)$$

$$k_q = 2.6 \times 10^{-11}\ \mathrm{cm^3\ molecule^{-1}\ s^{-1}} \qquad (8)$$

where the quenching quantum yield is $\phi_q = 1$.[14] The quantum yield for OH production ϕ_{OH} was obtained by measuring the relative intensity of the asymptotic OH signal to that produced in the reaction between $O(^1D)$ and H_2O,

$$H_2O + O(^1D) \rightarrow 2\ OH$$

$$k = 2.2 \times 10^{-10}\ \mathrm{cm^3\ molecule^{-1}\ s^{-1}} \qquad (9)$$

where the OH formation quantum yield is $\phi_{OH} = 2$.[14] The value of k_{total} was determined by the measurement of the temporal profiles of $O(^3P)$ and $O(^1D)$, where the signal intensity was plotted as a function of the delay between the photolysis and LIF laser pulses.

The experimental setup was essentially the same as that in the previous study.[15] The reaction cell ($60 \times 60 \times 60$ mm^3) was evacuated by a rotary pump through a liquid N_2 trap. Sample gas mixtures containing N_2O as the $O(^1D)$ source, HFC or N_2 as the reactant, and He as a buffer were flowed ($\sim$100 Torr cm^3 s^{-1}) through the reaction cell where the pressure was measured by a capacitance pressure gauge. The HFC, N_2O, N_2, and He gases were obtained commercially and used without further purification. The H_2O vapor was obtained from degassed, distilled water at room temperature. The $O(^1D)$ was generated in the reaction cell by the photolysis of N_2O at 193 nm. Since the translationally hot $O(^1D)$ atom is quickly thermalized by the collisions with buffer gas on a time scale of less than a microsecond under our experimental conditions, hot atom effects can be ignored.[16] The probe laser beam for the detection of $O(^1D)$ or reaction products was also introduced into the reaction cell after a time delay. The reaction time is defined as this delay time, t, between the photolysis and probe laser pulses, which was controlled by a pulse delay generator (Stanford Research, model DG535).

The $O(^1D)$ and $O(^3P_2)$ atoms were detected by LIF at 115.22 and 130.22 nm, respectively. The VUV laser light at 115.22 nm was generated by frequency tripling (3ω) of a dye laser (Lambda Physik, model FL3002) at 345.6 nm in Xe gas. The vuv laser light at 130.22 nm was generated by four-wave difference mixing ($2\omega_1 - \omega_2$) using two dye lasers (Lambda Physik, model FL3002 and Scanmate) in Kr gas. The dye laser output was frequency doubled by a BBO crystal for the ω_1 light of 212.56 nm, which was two-photon resonant with Kr $5p[^1/_2]_0$. The two dye lasers were pumped by a XeCl excimer laser (Lambda Physik, model Lextra-50). The wavelength of ω_2 was tuned around 578.1 nm. The laser beams were focused into a Xe or Kr gas cell with a lens with a focal length of 200 mm. The vuv laser light generated in the Xe or Kr gas cell was introduced into the reaction cell through a LiF window in a direction orthogonal to the photolysis laser direction. The intensity of the vuv light was monitored by the measurements in a photocurrent cell which contained nitric oxide (NO) gas. The photocurrent cell was located behind the reaction region. The LIF emission was detected by a photomultiplier tube (EMR, model 547 J-08-17) at right angles to the both photolysis and probe laser beams.

The $OH(X\ ^2\prod)$ radical was also detected by LIF around 282 nm using the dye laser pumped by the XeCl excimer laser. This laser beam was introduced into the reaction cell in a direction counterpropagated to the photolysis laser beam. The intensity of the beam was monitored by a photodiode. The LIF signals of OH(A−X) transition around 309 nm were separated by an interference filter (BARR Associates, Inc.; bandwidth = 12 nm) and detected by a dynode-gated photomultiplier tube (Hamamatsu, models 1P28 and C1392-56) with a high-speed amplifier (Hamamatsu, model C5594) to separate the resonance fluorescence and the strong laser scattering. The signal from the photomultipliers for the detection of $O(^1D)$, $O(^3P)$, and OH(X) was averaged by gated integrators (Stanford Research, SR250). The fluorescence decay curve of OH(A−X) was measured by using a digital oscilloscope (Tektronix, model TDS380P).

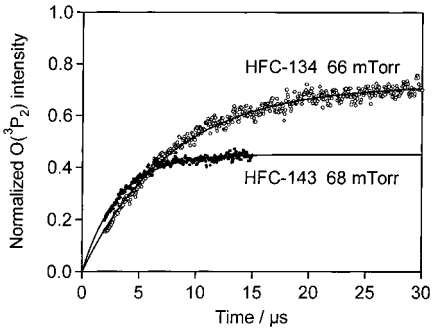

Figure 1. Temporal profiles of the $O(^3P_2)$ signal produced from CHF_2-CHF_2 (HFC-134) + $O(^1D)$ and CH_2FCHF_2 (HFC-143) + $O(^1D)$. The signal intensities are normalized by the asymptotic signal intensity of $O(^3P_2)$ produced from N_2 + $O(^1D)$. The $O(^1D)$ atoms are produced from the photodissociation of N_2O by 193 nm laser pulse at $t = 0$. The partial pressure of N_2O is kept constant (ca. 1 mTorr) in the reactions of HFC-134, HFC-143, and N_2. Helium gas is added (ca. 500 mTorr) as a buffer.

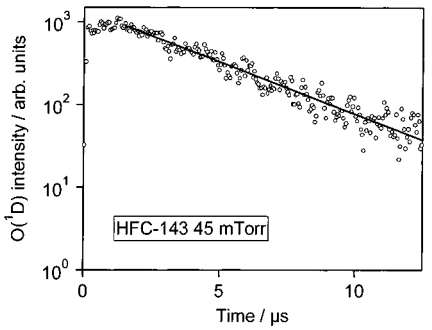

Figure 2. Temporal profile of $O(^1D)$ produced from the photodissociation of N_2O at 193 nm under the presence of 45 mTorr of CH_2FCHF_2 (HFC-143). The N_2O pressure is ca. 1 mTorr). Helium gas is added (ca. 500 mTorr) as a buffer.

3. Results

3.1. Total Rate Constants for the Removal of $O(^1D)$. Typical results of the temporal profiles of $O(^3P)$ and $O(^1D)$ are shown in Figures 1 and 2, respectively. Because the quenching rate of $O(^1D)$ by the He gas used as a buffer gas is extremely slow ($<5 \times 10^{-14}$ cm^3 molecule^{-1} s^{-1}),[17] the quenching process of $O(^1D)$ by He can be neglected here. The rise and decay rates k, obtained by a least-squares fit, were measured at different pressures in the reaction cell, because they are the function of reactant concentrations, i.e.,

$$k = k_{HFC}[HFC] + k_{N_2O}[N_2O] + k_{diff} \qquad (10)$$

where k_{N_2O} and k_{HFC} are the second-order rate constants for the removal of $O(^1D)$ by the reactants N_2O and HFC, respec-

TABLE 1: Rate Constants in the Reaction of O(^{1}D) with HFC (Units in 10^{-11} cm^3 molecule^{-1} s^{-1})

	k_{total}					
reactant	O(^{1}D) decay[a]	O(^{3}P) rise[b]	k_q	k_{OH}	k_{other}	ref
CF_3-CF_3 (CFC-116)	0.015 (±0.003)	−	0.013 (±0.003)			25
CHF_2-CF_3 (HCF-125)	−	1 (+1/−0.5)	0.2 (+0.2/−0.1)	0.6 (+0.6/−0.3)	0.2(±0.2)	this work
	12.3 (±0.6)	−	−	$k_{OH} + k_{other} = 1.8(+2.8/-1.8)$		10
		−	−	$k_{OH} + k_{other} = 4.6(\pm 1.2)$[c]		18
CH_2F-CF_3 (HFC-134a)	4.9(±0.5)	−	3.2(±0.5)	1.2(±0.3)	0.5(±0.3)	this work
	4.85(±0.25)	−	−	$k_{OH} + k_{other} = 0.3$ (±0.3)		10
CHF_2-CHF_2 (HFC-134)	3.9(±0.4)	4 (±1)	2.8(±0.5)	1.0(±0.3)	0.1 (+0.3/−0.1)	this work
CH_3-CF_3 (HFC-143a)	4.0 (±0.5)	5 (±1)	0.7(±0.2)	1.5(±0.3)	1.8(±0.4)	this work
	−	−	−	$k_{OH} + k_{other} = 10(\pm 2)$[c]		18
CH_2F-CHF_2 (HFC-143)	11 (±1)	12 (±2)	5.0(±0.8)	2.0(±0.5)	4.1(±0.9)	this work
CH_3-CHF_2 (HFC-152a)	−	15 (±2)	5.1 (±1.1)	2.3(±0.5)	7.6(±1.4)	this work
	20.2(±1.5)	−	−	$k_{OH} + k_{other} = 9.3(\pm 1.6)$		10

[a] Determined from the decay curve of O(^{1}D) signal. [b] Determined from the rise curve of O(^{3}P) signal. [c] Using the currently recommended value of the rate constant for O(^{1}D) + N_2O of 1.16×10^{-10} cm^3 molecule^{-1} s^{-1}.[14]

TABLE 2: Branching Ratios in the Reaction of O(^{1}D) with HFC

reactant	ϕ_q	ϕ_{OH}	ϕ_{other}	ref
CF_3-CF_3 (CFC-116)	0.85(±0.15)	−	0.15(±0.15)	25
CHF_2-CF_3 (HFC-125)	0.24(±0.04)	0.6(±0.1)	0.2(±0.1)	this work
	0.85(+0.15/−0.22)	−	−	10
CH_2F-CF_3 (HFC-134a)	0.65(±0.06)	0.24(±0.04)	0.11(±0.07)	this work
	0.94(+0.06/−0.10)	−	−	10
CHF_2-CHF_2 (HFC-134)	0.72(±0.10)	0.25(±0.06)	0.03 (−0.03/+0.12)	this work
CH_3-CF_3 (HFC-143a)	0.18(±0.04)	0.38(±0.06)	0.44(±0.07)	this work
CH_2F-CHF_2 (HFC-143)	0.45(±0.06)	0.18(±0.04)	0.37(±0.07)	this work
CH_3-CHF_2 (HFC-152a)	0.34(±0.06)	0.15(±0.02)	0.51(±0.06)	this work
	0.54(±0.07)			10

tively, [N_2O] and [HFC] are the concentrations of N_2O and HFC, respectively, and k_{diff} corresponds to effects of the diffusion from the viewing zone for the reactants and products. The plots of the O(^{1}D) decay rates and the O(^{3}P) rise rates vs the HFC-143 concentration are shown in Figure 3. The rate constant obtained from the slope of the O(^{1}D) decay rate plots is $(1.2 \pm 0.2) \times 10^{-10}$ cm^3 molecule^{-1} s^{-1}, while that from the O(^{3}P) rise rate plots is $(1.1 \pm 0.1) \times 10^{-10}$ cm^3 molecule^{-1} s^{-1}. The relatively large intercepts of both plots for the O(^{1}D) decay and O(^{3}P) rise rates in Figure 3 are mainly due to the diffusion, that is, k_{diff} in eq 10. The diameters of the photolysis and probe laser beams were both ca. 1 mm. The escape time out of the overlap region of these laser beams is estimated to be about $\sim 10^{-6}$ s with these beam diameters. The rate constants of O(^{1}D) with the various HFC reactants obtained in this study from the plots of O(^{1}D) decay and/or O(^{3}P) rise rates are listed in Table 1. For HFC-134, HFC-143a, and HFC143, the total reaction rate constants were obtained by measuring both O(^{1}D) decay and O(^{3}P) rise. The values determined by the two different methods are in agreement with each other within their experimental uncertainties for all of the three compounds.

3.2. Quantum Yields for the O(^{3}P) Production. The temporal profiles of O($^3P_2$) formed in the reaction of O(^{1}D) with HFC were measured. Since the intramultiplet relaxation rate by collision is fast enough,[15] the distributions among the spin−orbit states $j = 2$, 1, and 0 of O(^3P_j) should be completely thermalized in a time scale of less than a micro-second under our experimental conditions.[15] The thermal population at room temperature is [O($^3P_2$)]:[O($^3P_1$)]:[O($^3P_0$)] = 1:0.282:0.068. Therefore, the measured O($^3P_2$) signal intensity is proportional to the total concentration of spin−orbit states of O(^{3}P). When the delay time is long enough to quench O(^{1}D) completely, the signal intensity of O(^{3}P) approaches an asymptotic value. Since N_2 quenches O(^{1}D) to O(^{3}P) with unit efficiency, the asymptotic signal intensity measured in the reaction HFC + O(^{1}D) is compared with that in the reaction N_2 + O(^{1}D) keeping the initial O(^{1}D) concentration constant. The ratio obtained by this comparison is the quantum yield, ϕ_q, for the electronic quenching of O(^{1}D). The removal by the reaction of O(^{1}D) with N_2O was estimated according to the concentrations and the reported rate constant of $k_{N_2O} = 1.16 \times 10^{-10}$ cm^3 molecule^{-1} s^{-1}.[14] In the present experiments, the ratio of $k_{N_2O}[N_2O]$ to k_{HFC}[HFC] in eq 10 was kept less than 10% and was taken into account in the calculations of ϕ_q. The values of ϕ_q thus measured are listed in Table 2 with literature values for C_2F_6. The values of the rate constant k_q for the quenching path calculated with expression (4) are summarized in Table 1.

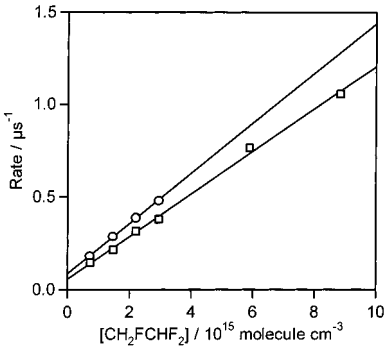

Figure 3. Plots of the measured decay rates of O(^{1}D) (circles) and rise rates of O(^{3}P) (squares) as a function of the concentration of CH_2-$FCHF_2$ (HFC-143).

3.3. Quantum Yields for the OH Production. In the reactions between O(^{1}D) and HFCs, OH radicals are generated. For the determination of the quantum yield for OH radicals produced in the reactions of O(^{1}D) with HFCs, the temporal profile of the OH signal was also observed in the present study with the exciting laser wavelength fixed at the $Q_1(2)$ line of the A−X 1−0 transition. The signal intensity of OH approached an asymptotic value. This asymptotic OH signal was also normalized by the method similar to that used in the quantum

yield measurements of $O(^3P)$ production. Since the reaction rates of $O(^1D)$ with HFCs are over 10^3 times larger than those of OH + HFCs,[14] the decay of OH radicals due to the secondary reactions can be ignored. However, the quenching of OH(A) radicals excited by the LIF laser must be considered. Actually, the fluorescence lifetimes of OH(A−X) observed in the present study were shorter (300−600 ns) than the natural radiation lifetime (≈700 ns) of OH(A). The fluorescence quantum yield of OH(A) ϕ_f is given by

$$\phi_f = \frac{\tau_f}{\tau_0} \tag{11}$$

where τ_f and τ_0 are the observed fluorescence and the natural radiation lifetimes, respectively. Therefore, the quantum yield for the OH production is given by

$$\phi_{OH} = 2\frac{I_{asy}^{HFC}}{I_{asy}^{H_2O}}\frac{\tau_f^{H_2O}}{\tau_f^{HFC}} \tag{12}$$

where I_{asy}^{HFC} and $I_{asy}^{H_2O}$ are the observed asymptotic intensities of the OH signal formed in the reaction HFC + $O(^1D)$ and that of the OH signal formed in the reaction H_2O + $O(^1D)$, respectively. $\tau_f^{H_2O}$ and τ_f^{HFC} are the fluorescence lifetimes measured under the experimental condition of the reaction H_2O + $O(^1D)$ and HFC + $O(^1D)$, respectively. The values of ϕ_{OH}, and ϕ_{other} (= 1 − ϕ_q − ϕ_{OH}) obtained in this study are summarized in Table 2 with the literature values for C_2F_6. The values of the rate constants, k_{OH} and k_{other}, calculated with expressions (5) and (6) are summarized in Table 1.

4. Discussion

Warren et al.[10] measured the k_{total} values with HFCs using time-resolved vuv atomic resonance fluorescence detection of $O(^3P)$ with an oxygen lamp after the photolysis of O_3 by a KrF laser pulse (248 nm), and obtained the ϕ_q values by measuring the ratios of the asymptotic fluorescence signal level between the HFCs and N_2. The results reported by Warren et al.[10] are also listed in Tables 1 and 2. The total rate constants obtained in this study are in good agreement with those reported by Warren et al. for CH_2FCF_3 (HFC-134a) and CH_3CHF_2 (HFC-152a) (Table 1). However, for $O(^1D)$ + CHF_2CF_3 (HFC-125), our value of the total rate constant is about 10 times smaller than their value. The reason for the difference is not clear. The rate constant reported by Warren et al. for CHF_2CF_3 (HFC-125) is even 2 times larger than that for CH_2FCF_3 (HFC-134a). It is more likely that the rate constant for CHF_2CF_3 (HFC-125) which has one H atom is smaller than that for CH_2FCF_3 (HFC-134a) which has two H atoms, since C_2F_6 is almost nonreactive with $O(^1D)$ (Table 1). The ϕ_q value of 0.24 ± 0.02 for HFC-125 in this study is much smaller than the value of 0.85 + 0.15/−0.22 reported by Warren et al.[10] (Table 2). The OH formation quantum yield of 0.6 ± 0.1 for $O(^1D)$ + HFC-125 measured in this study indicates that the ϕ_q value for HFC-125 should be less than 0.4. Our small ϕ_q value of 0.24 for HFC-125 is consistent with the measured ϕ_{OH} value. The ϕ_q values for HFC-134a and HFC-152a are a little smaller than those reported by Warren et al.[10] (Table 2). The ϕ_{OH} value of 0.24 ± 0.02 measured in this study supports our ϕ_q value of 0.65 and indicates that the value of 0.94 by Warren et al.[10] is too large.

Green and Wayne[18] measured the loss rate of the HFC reactants relative to loss rate of N_2O by $O(^1D)$ atoms from NO_2 with irradiation of a continuous cadmium lamp (229 nm), detecting the infrared absorption intensities of the HFC and N_2O as a function of time. Table 2 also lists the k_{OH} + k_{other} values which are calculated from the results reported by them, using the currently recommended value of the rate constant for $O(^1D)$ + N_2O of 1.16×10^{-10} cm^3 molecule^{-1} s^{-1}.[14] The values of k_{OH} + k_{other} calculated from their results for HFC-125 and HFC-143a are several times larger than our values of k_{OH} + k_{other} and even larger than the total rate constants obtained in this study.

Note that the k_{OH} values are proportional to the total number of H atoms included in the HFC molecule. This means that the attack of $O(^1D)$ on the C−H bond of HFC gives rise to the chemical reaction to produce the OH radical. That is consistent with other numerous other studies[19−43] where the mechanisms of H atom abstraction by $O(^1D)$ and of $O(^1D)$ atom insertion into a C−H bond have been suggested. Luntz[19] concluded that the insertion dominates for small hydrocarbons while the abstraction becomes an increasingly important source of OH as the size of the hydrocarbon increases.

The C−H bond fission, C−C bond fission, and HF molecule elimination accompanied by C−O bond formation are expected as the reaction pathway(s) for k_{other} (= k_{total} − k_{OH} − k_q) in the reactions of HFCs + $O(^1D)$. The reaction mechanism of C_2H_6 + $O(^1D)$ has been investigated,[19−22] in which the C−C bond cleavage have been suggested to be a dominant reaction pathway. Park and Wiesenfeld[22] reported that the quantum yield for the OH formation in the reaction of C_2H_6 + $O(^1D)$ was 0.033, while it was near unity in the reaction of CH_4 + $O(^1D)$. Analogous to the discussion on the C_2H_6 + $O(^1D)$ reaction, the C−C bond fission process is the most feasible as the reaction pathway for k_{other} in the reactions of HFCs + $O(^1D)$.

Another possibility of the main reaction pathway which is responsible for k_{other} is the HF formation process, since the infrared emissions from the vibrationally excited HF molecules were observed in the reaction of $O(^1D)$ with CHF_3 and CH_3F.[23,24] However, we have not succeeded in explaining the trend of k_{other} by counting the numbers of adjacent H−F combinations in the HFC reactants. Anyway, further experiments are required to identify the reaction pathway(s) for k_{other} and to understand the dependence of k_{other} on the HFC reactants.

Since C_2F_6 is quite inert to the quenching of $O(^1D)$ (Table 1), the interaction of $O(^1D)$ on the H site of HFCs seems to affect the physical quenching as well as the OH formation. The quenching rate constants, however, seem to depend neither on the number of included H atoms nor on the molecular structure. Probably, the position and shape at the seam of the singlet and triplet potential energy surfaces of the intermediate complex in the HFCs + $O(^1D)$ reaction may affect the k_q values. These factors may not be simply related to the structure of the HFC reactants.

If the intermediate complex formed in the reaction process of HFC + $O(^1D)$ is decomposed statistically, the product branching ratios to the OH formation, the C−C bond fission, and HF formation can be predicted by statistical theories such as RRKM calculations. However, we did not perform the estimation of the reaction branching using the RRKM theory, because the many parameters, e.g., bond energies and normal-mode frequencies of the complexes, which were required in the RRKM calculations were not available for the reaction systems of HFCs + $O(^1D)$. In the reaction of C_2H_6 + $O(^1D)$, Luntz[19] measured the vibrational and rotational distributions of OH products and found that the distributions were different from the predictions by the statistical theory. This suggests that the

statistical calculations may not be effective in the HFCs + O(^{1}D) reaction systems.

Acknowledgment. This work was supported by International Joint Research Grants of the New Energy and Industrial Technology Development Organization (NEDO). This work was also partly supported by Grants-in-Aid from the Ministry of Education, Science, and Culture of Japan. The authors thank M. Kawasaki in Kyoto University and K. Takahashi in the Solar Terrestrial Environment Laboratory for their helpful discussions.

References and Notes

(1) Molina, M. J.; Rowland, F. S. *Nature* **1974**, *249*, 810.
(2) Rowland, F. S.; Molina, M. J. *Rev. Geophys. Space Phys.* **1975**, *13*, 1.
(3) Farman, J. D.; Gardiner, B. G.; Shanklin, J. D. *Nature* **1985**, *315*, 207.
(4) Solomon, S. *Nature* **1990**, *347*, 6291.
(5) World Meteorolical Organization. Atmospheric Ozone 1989, Scientific Assesment of Straspheric Ozone. Report No. 20; Vol. II, Appendix: AFEAS Report; WMO Global Research and Monitoring Project: Geneva, 1989.
(6) *Progress and Problems in Atmospheric Chemistry*; Baker, J. R., Ed.; World Scientific: Singapore, 1995.
(7) Finlayson-Pitts, B. J.; Pitts, J. N., Jr. *Chemistry of the Upper and Lower Atmosphere: Theory, Experiments, and Applications*; Academic Press: San Diego, 1999.
(8) Houghton, J. T.; Meria Filho, L. G.; Callander, B. A.; Harris, N.; Kattenberg, A.; Maskell, K. *Climmate Change 1995: The Science of Climate Change*; Lakeman, J. A., Ed; Cambridge University Press: Cambridge, 1996.
(9) Cvetanoviæ, R. J. *Can. J. Chem.* **1974**, *52*, 1452.
(10) Warren, R.; Gierczak, T.; Ravishankara, A. R. *Chem. Phys. Lett.* **1991**, *183*, 403.
(11) Takahashi, K.; Wada, R.; Matsumi, Y.; Kawasaki, M. *J. Phys. Chem.* **1996**, *100*, 10145.
(12) Preston, K. F.; Barr, R. F. *J. Chem. Phys.* **1971**, *54*, 3347.
(13) Zhu, Y. F.; Gordon, R. J. *J. Chem. Phys.* **1990**, *92*, 2897.
(14) DeMore, W. B.; Sander, S. P.; Golden, D. M.; Hampson, R. F.; Kurylo, M. J.; C. J. Howard, Ravishankara, A. R.; Kolb, C. E.; Molina, M. J. *Chemical Kinetics and Photochemical Data for Use in Stratospheric Modeling*; Jet Propulsion Laboratory Publication 97-4; NASA, California Institute of Technology: Pasadena, CA, 1997; Vol. 12,
(15) Abe, M.; Sato, Y.; Inagaki, Y.; Matsumi, Y.; Kawasaki, M. *J. Chem. Phys.* **1994**, *101*, 5647.
(16) Matsumi, Y.; Shamsuddin, S. M.; Sato, Y.; Kawasaki, M. *J. Chem. Phys.* **1994**, *101*, 9610.
(17) Stief, L. J.; Payne, W. A.; Klemm, R. B. *J. Chem. Phys.* **1975**, *62*, 4000.
(18) Green, R. G.; Wayne, R. P. *J. Photochem.* **1977**, *6*, 371.
(19) Luntz, A. C. *J. Chem. Phys.* **1980**, *73*, 1143.
(20) Andresen, P.; Luntz, A. C. *J. Chem. Phys.* **1980**, *72*, 5842.
(21) Andresen, P.; Luntz, A. C. *J. Chem. Phys.* **1980**, *72*, 5851.
(22) Park, C. R.; Wiesenfeld, J. R. *J. Chem. Phys.* **1991**, *95*, 8166.
(23) Burks, T. L.; Lin, M. C. *Chem. Phys.* **1978**, *33*, 327.
(24) Aker, P. M.; Niefer, B. I.; Sloan, J. J.; Heydtmann, H. *J. Chem. Phys.* **1987**, *87*, 203.
(25) Ravishankara, A. R.; Solomon, S.; Turnipseed, A. A.; Warren, R. F. *Science* **1993**, *259*, 194.
(26) Schmoltner, A. M.; Talkdar, R. K.; Warren, R. F.; Mellouki, A.; Goldfarb, L.; Gierczak, T.; McKeen, S. A.; Ravishankara, A. R. *J. Phys. Chem.* **1993**, *97*, 8976.
(27) Rudich, Y.; Hurwit, Y.; Frost, G. J.; Vaida, V.; Naaman, R. *J. Chem. Phys.* **1993**, *99*, 4500.
(28) Arai, H.; Kato, S.; Koda, S. *J. Phys. Chem.* **1994**, *98*, 12.
(29) Schott, R.; Schlütter, J.; Olzmann, M.; Kleinermanns, K. *J. Chem. Phys.* **1995**, *102*, 8371.
(30) Park, C. R.; Wiesenfeld, J. R. *Chem. Phys. Lett.* **1991**, *186*, 170.
(31) Casavecchia, P.; Buss, R. J.; Sibener, S. J.; Lee, Y. T. *J. Chem. Phys.* **1980**, *73*, 6351.
(32) Satyapal, S.; Park, J.; Bersohn, R.; Katz, B. *J. Chem. Phys.* **1989**, *91*, 6873.
(33) Lin, J. J.; Harich, S.; Lee, Y. T.; Yang, X. *J. Chem. Phys.* **1999**, *110*, 10821.
(34) González, M.; Hernando, J.; Baños, I.; Sayós, R. *J. Chem. Phys.* **1999**, *111*, 8913.
(35) González, M.; Puyuelo, M. P.; Hernando, J.; Sayós, R.; Enríquez, P. A.; Guallar, J.; Baños, I. *J. Phys. Chem. A* **2000**, *104*, 521.
(36) Turumaki, H.; Fujimura, Y.; Kajimoto, O. *Chem. Phys. Lett.* **1999**, *301*, 145.
(37) Yamazaki, H.; Cvetanoviæ, R. J. *J. Chem. Phys.* **1964**, *41*, 3703.
(38) Michaud, P.; Cvetanoviæ, R. J. *J. Chem. Phys.* **1972**, *76*, 1375.
(39) Paraskevopoulos, G.; Cvetanoviæ, R. J. *J. Chem. Phys.* **1969**, *50*, 590.
(40) Paraskevopoulos, G.; Cvetanoviæ, R. J. *J. Chem. Phys.* **1970**, *52*, 5821.
(41) Lin, C. L.; DeMore, W. B. *J. Phys. Chem.* **1973**, *77*, 863.
(42) DeMore, W. B.; Raper, O. F. *J. Chem. Phys.* **1967**, *46*, 2500.
(43) Jayanty, R.; Simonaitis, R.; Heicklen, J. *Int. J. Chem. Kinet.* **1976**, *8*, 107.